2nd International Engineering Mechanics and Materials Specialty Conference
le 2è Congrès international de mécanique et des matériaux

Ottawa, Ontario
June 14-17, 2011 / 14 au 17 juin 2011

Cylindrical Concrete Tanks with a Conical Base – Internal Force Discrepancies Between Different Analysis Tools

Mark Bruder
R.V. Anderson Associates Limited, Toronto, Ontario, Canada

Abstract: In the design of cylindrical concrete tanks, it is crucial for the designer to choose and correctly apply an appropriate analysis tool. Two well-known analysis tools are 1) a publication by the Portland Cement Association (1993) entitled "*Circular Concrete Tanks Without Pre-stressing*" (CCT), and 2) a finite element analysis (FEA) with a three-dimensional model built in a software program such as SAP2000. When comparing these tools, internal force discrepancies (IFD) exist. While CCT does not advise on self-weight loading, soil-structure interaction, and changes in base geometry, FEAs can incorporate these components. This paper presents a study of nine cylindrical concrete tanks where internal forces strictly in the tank wall are obtained from FEAs and CCT. Various combinations of loads and wall-base boundary conditions are considered. Comparisons between resultant internal forces from FEAs and CCT are made to investigate the potential range of IFD. It was found that high IFD exist when the CCT wall-base joint is fixed with horizontal deflection restrained and IFD are reduced when the wall-base joint is hinged. For designers, it is recommended that an FEA be employed if the shape, load cases, and assumed boundary conditions of the tank in question fall outside the parameters outlined by CCT. Otherwise, the resultant internal forces may lead to an inadequate design.

1. INTRODUCTION

In the design of cylindrical concrete tanks, it is crucial for the designer to choose and correctly apply an appropriate analysis tool. Tanks that are used as digesters in wastewater treatment plants must be designed to withstand all applied loads and meet high serviceability requirements for water tightness. Two well-known analysis tools are 1) a publication by the Portland Cement Association (1993) entitled "*Circular Concrete Tanks Without Pre-stressing*" (CCT), and 2) a finite element analysis (FEA) with a three-dimensional model built in a software program such as SAP2000. A designer may employ CCT exclusively or as a first approximation prior to utilizing an FEA. When comparing these tools, discrepancies in internal forces exist due to analysis assumptions and simplifications, inherent differences in analysis methodologies, and design specific applicability.

In two FEA case studies, El Mezaini (2004, 2006) investigated how self-weight loading, soil-structure interaction, and changes in base geometry affect the internal forces of cylindrical concrete tanks. It was demonstrated that significant discrepancies exist in maximum internal forces and deflections in the wall and base slab of a given tank when comparing FEAs to CCT. For example, the deviation between the FEA relative to CCT was as high as 59% for maximum ring tension and -151% for maximum bending moment forces in the wall for a medium soil stiffness. Since El Mezaini studied a single tank size, it cannot be determined whether the discrepancies found are generally consistent for commonly used tank sizes or merely outliers of a special case.

Self-weight loading, soil-structure interaction, and changes in base geometry are not integrated into CCT design tables. If the designer deems these elements essential inclusions in the analysis, it is important to be aware of how the internal forces might differ between an FEA and CCT.

This paper expands on El Mezaini's research with a study of nine cylindrical concrete tanks. Internal forces strictly in the tank wall are obtained from FEAs and CCT. Various combinations of loads and wall-base boundary conditions are considered. Comparisons between resultant internal forces from FEAs and CCT are made to investigate the potential range of internal force discrepancies (IFD). Discussed within is a summary of chosen tank sizes, loading combinations, analysis assumptions, and results. It is hoped that this data will aid designers by highlighting some of the differences between analysis tools.

2. BRIEF BACKGROUND

Regarding the effects of self-weight loading, soil-structure interaction, and changes in base geometry on the design of cylindrical concrete tanks, El Mezaini (2004, 2006) concluded the following:

- Cylindrical tanks are sensitive to self-weight loading. Greater settlement under the wall, as compared to the center of the tank, leads to larger than expected internal forces in the wall. This may be inadvertently overlooked by engineers.
- Settlement is proportional to the sub-base soil stiffness. The softer the soil is, the greater the wall will settle.
- Rotation of the base slab is transferred to the wall through the wall-base rigid joint. A conical base slab exhibits less differential settlement due to its rigidity. However, as the slab is flattened under the applied loads, the wall-base is pushed outward, which increases ring tension forces in the wall.

Considering these conclusions, it would appear that self-weight loading, soil-structure interaction, and changes in base geometry are essential components to consider in the design of cylindrical concrete tanks. Thus, if a designer wishes to employ CCT exclusively, they should be aware of the potential range of IFD that exist for an assortment of tank sizes.

3. TANK SHAPES AND SIZES

For concrete digester tanks in wastewater treatment plants, common round shapes include the pancake (short cylinder) and the egg. Depending on process design requirements, either a fixed or floating cover may be employed. For this paper, a short cylindrical digester tank with a conical base and a removable floating cover is considered. In choosing the various tank sizes for this investigation, some recommendations from the published literature were followed as per Table 1. Table 2 shows the chosen cylindrical tank sizes.

Table 1: Summary of cylindrical digester tank size recommendations

	Wall Height, H [m]	Diameter, D [m]	Base Slab Slope
WEF & ASCE/EWRI (2010)	6.0 – 14.0	8.0 – 40.0	1V:3H – 1V:6H
Metcalf & Eddy (1991)	7.5 – 14.0	6.0 – 38.0	1V:4H

Table 2: Chosen cylindrical tank sizes *

Tank #	1	2	3	4	5	6	7	8	9
Height, H [m]	10.5	9	8.4	8	8	8	7.5	7	6
Diameter, D [m]	21	27	21	24	20	16	18.75	21	12
Thickness, t [m]	0.5	0.5	0.5	0.5	0.5	0.5	0.5	0.5	0.5
H^2/Dt	10.5	6	6.72	5.33	6.4	8	6	4.67	6
D/H	2	3	2.5	3	2.5	2	2.5	3	2

* Category: 1 – height, 2 – diameter, 3 – H^2/Dt. See following paragraph for discussion.

In Table 2, the tank heights and diameters fall within the ranges specified in Table 1. The tanks are numbered from largest to smallest height and are divided into three categories. The first category is for tanks 4, 5, and 6 with a height of 8 m. The second is for tanks 1, 3, and 8 with a diameter of 21 m. The third is for tanks 2, 7, and 9 with H^2/Dt equal to 6 (H^2/Dt is a dimensionless ratio used in CCT). Within each category, tanks have D/H ratios of 2, 2.5, or 3 (a common range for the pancake tank shape).

Figures 1 and 2 show a typical tank diagram and example finite element model (FEM), respectively. The base slab has a 1V:4H slope with a 1 m diameter flat centre. CCT assumes that tanks have an entirely flat base slab. This clear difference in base slab geometry and stiffness leads to IFD.

A consistent thickness of 500 mm for the wall and base slab facilitates a simplified FEM. To ensure the self-weight loading was reasonable, this thickness was examined for design practicality. Prior to finalizing the tank sizes, a crack control check was performed as outlined by CCT to investigate the induced concrete tensile stress in the walls from dry shrinkage. For all tanks, the maximum tensile stress was found to be less than the assumed allowable tensile strength equal to 10% of the concrete compressive strength. Thus, 500 mm is a suitable wall and base slab thickness for the purposes of this study.

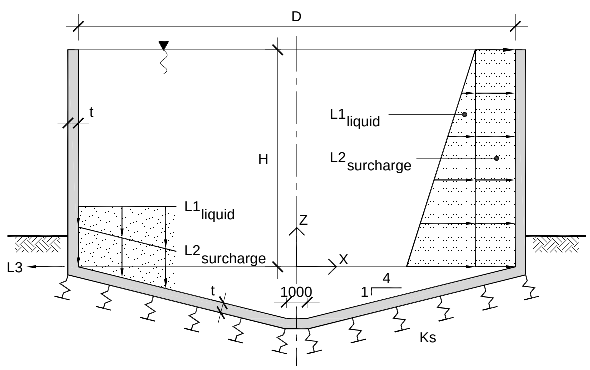

Figure 1: Typical tank diagram

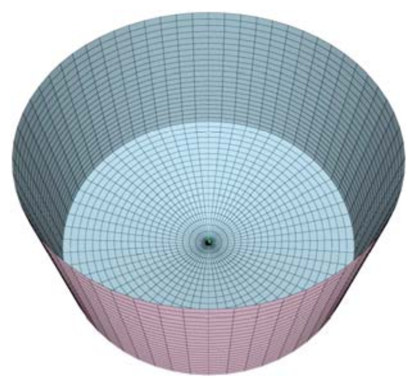

Figure 2: Example FEM

4. MODELS

The American Concrete Institute published ACI 318 (ACI 2005) regarding building code requirements for reinforced concrete and ACI 350 (ACI 2006) to assist in the design and construction of environmental concrete structures. These codes are referenced by CCT for loading scenarios and factors. Typically, in water and wastewater treatment plants, cylindrical concrete tanks are partially buried. As per ACI 318, the passive resistance of the backfill cannot be used to resist the applied loads from within the tank. In this paper, only loads from within the tank are considered and it is assumed that the tank has not yet been backfilled. All tanks were analyzed with a single sub-base soil condition: a medium soil stiffness with the coefficient of sub-grade reaction (K_S) taken as 50,000 kN/m³.

The tanks were analyzed with various combinations of the following loads:

- S_W) Self-weight of the tank: dead load of the wall and base slab.
- L1) Liquid Pressure, Triangular: the tank is filled to the top with liquid.
- L2) Surcharge Pressure, Rectangular: air trapped within from the floating tank cover.
- L3) Base Shear: correction load from CCT, see last paragraph of section 4 for explanation.

From CCT, four models were considered with load case and boundary condition scenarios:

- C1) CCT Section 7: Free Top & Fixed Base, Triangular Load (L1).
- C2) CCT Section 8: Free Top & Hinged Base, Triangular Load (L1).
- C3) CCT Section 9: Free Top & Hinged Base, Trapezoidal Load (L1+L2).
- C4) CCT Section 11: Free Top & Hinged Base, Trapezoidal Load (L1+L2) + Base Shear (L3).

For the FEAs, two models were considered with load case and boundary condition scenarios:

F1) Free Top & Continuous Base Joint, Self-weight (S_W) + Triangular Load (L1).
F2) Free Top & Continuous Base Joint, Self-weight (S_W) + Trapezoidal Load (L1+L2).

Both FEA models were built with a continuous wall-base joint that is free to displace, rotate, and distribute moment. In CCT, the tank analysis is simplified by idealizing the wall-base joint as either totally fixed or hinged with no horizontal displacement allowed. The reactions computed for the wall can then be applied to the base slab as an approximate solution. Since a perfectly fixed wall-base joint is unlikely, the presence of model C1 in this study is for comparative purposes only. If the base of the wall were free to slide outward, then shear forces at the wall-base joint could not develop. With a continuous wall-base joint, as with models F1 and F2, the base slab provides resistance against horizontal displacement of the wall. Thus, any shear force applied at the base between a perfectly fixed or fully unrestrained wall-base joint is a reasonable estimate. Model C4 simulates this as advised by CCT.

5. ANALYSIS TOOLS

5.1. Circular Concrete Tanks (CCT)

CCT outlines a sequential, step-by-step procedure for determining internal design forces. In summary, the designer calculates the dimensionless ratio H^2/Dt, chooses appropriate loads and boundary conditions, references tables to find coefficients corresponding to a given wall height, then calculates the internal forces. Guidance is given for crack control, load factors, ACI sanitary coefficients, reinforcement design, effects of varying wall thickness, temperature variation in the tank wall, and base slab design.

5.2. Finite Element Analysis (FEA)

Each FEM is composed of a three-dimensional shell element mesh. To facilitate good stress results, the aspect ratio (length over height) for shell elements was kept between 1 and 3 with a constant height of 500 mm. To incorporate the sub-base soil condition, compression-only springs were applied perpendicular to element joints in the base slab. The spring constant (K_S) was set to 50,000 kN/m³. The loads L1 and L2 were applied to the inside face of the shell elements. Load factors and sanitary coefficients were applied as per CCT recommendations. The average convergence of internal joint forces was found to be approximately 2% indicating that the FEMs are sufficiently accurate. While CCT uses the internal diameter in the calculation of H^2/Dt (see Figure 1), the FEMs were built with the chosen tank diameters at the wall centre lines. It is possible that this difference could lead to IFD.

In practice, tanks with a floating cover must be constructed with a high out-of-roundness tolerance so the cover can move freely. Typically, digester steel cover manufacturers try to keep out-of-roundness below 50 mm. To achieve this in all tank FEMs, a central angle of 6º between elements was required. Note that under axi-symmetric loading and boundary conditions, it may not be necessary to model the entire tank structure. In this case, only a segment of the tank could be modeled, such as a quarter, with appropriate loads and boundary conditions.

6. RESULTS AND DISCUSSION

To give context to which IFD in the wall are notable, it will be discussed how the force diagrams are used in the wall design. Essentially, the bending moment and ring tension forces, resisted by vertical and horizontal reinforcement, respectively, must be contained within a reinforcing "envelope". This may be divided into upper and lower sections of the wall. In the upper section, forces are small and little reinforcement is needed. In the lower section, forces are larger and require larger rebar with tight spacing. It is not economical to step the reinforcement numerous times. Hence, for design purposes, the reinforcement required for the largest force is typically used throughout the entire lower section of the wall regardless of whether the forces are idealized to go to zero at the wall-base joint.

Table 3 below compares maximum internal forces in the wall from model "C" to model "F".

Table 3: Comparison of maximum internal forces in the wall

	Maximum Bending Moment (KN-m/m')									
Model	F1	C1	IFD%*	C2	IFD%*	F2	C3	IFD%*	C4	IFD%*
Tank #	(SW+L1)	(L1)	(F1, C1)	(L1)	(F1, C2)	(SW+L1+L2)	(L1+L2)	(F2, C3)	(L1+L2+L3)	(F2, C4)
1	129	-309	-142	114	13	135	125	8	62	120
2	130	-310	-142	129	1	137	143	-4	73	90
3	105	-232	-145	103	2	112	106	5	54	107
4	110	-245	-145	103	6	116	116	0	58	100
5	97	-208	-147	86	14	103	96	7	49	110
6	90	-170	-153	66	36	93	74	26	38	146
7	90	-179	-150	75	21	93	84	10	43	117
8	89	-185	-148	79	12	95	90	5	45	112
9	62	-92	-168	38	62	62	44	39	23	175
Average			-149		19			11		120
StDev**			8		18			13		25

	Maximum Ring Tension (KN/m')									
Model	F1	C1	IFD%*	C2	IFD%*	F2	C3	IFD%*	C4	IFD%*
Tank #	(SW+L1)	(L1)	(F1, C1)	(L1)	(F1, C2)	(SW+L1+L2)	(L1+L2)	(F2, C3)	(L1+L2+L3)	(F2, C4)
1	2546	1950	31	2338	9	2823	2643	7	2648	7
2	2441	1802	35	2254	8	2790	2634	6	2718	3
3	1917	1364	41	1686	14	2194	1969	11	2018	9
4	1924	1346	43	1729	11	2232	2074	8	2148	4
5	1717	1215	41	1509	14	1969	1778	11	1833	7
6	1488	1062	40	1287	16	1695	1511	12	1515	12
7	1515	1043	45	1305	16	1748	1570	11	1616	8
8	1469	978	50	1282	15	1727	1578	10	1646	5
9	851	534	59	668	27	999	839	19	860	16
Average			43		14			11		8
StDev.**			7		5			4		4

* Internal force discrepancy: percent deviation of model "F" as compared to "C".
** Standard deviation of the sample in percentage points.

As shown in Table 3, on average the maximum forces from model F2 are 15% larger than F1 for ring tension and 5% larger than F1 for bending moment. This is strictly the result of the additional surcharge pressure (L2) from a floating tank cover in model F2. Notice that in all model comparisons, for bending moment and ring tension, the largest IFD are found in tank 9 (the smallest tank size) and the smallest IFD are typically found in either tank 1 or 2 (the largest tank size). This suggests that the effects of self-weight loading, soil-structure interaction, and changes in base geometry on IFD are inversely proportional to the tank size. However, the three aforementioned effects are not necessarily the primary cause of this conclusion, as imperfections in the FEM and the potential inaccuracy of the FEA are likely candidates.

Figures 3 to 6 show internal force diagrams of tanks 1 and 9. Notice that for CCT and FEA comparisons, the shapes of the bending moment and ring tension force diagrams are in reasonably good agreement. The exceptions are found between the wall-base joint and, typically, the bottom third of the tank wall. Force diagrams for tanks 2 through 8 have not been included because their shapes are similar to tank 1. For models C2 and C3, with a hinged wall-base joint, the bending moment and ring tension go to zero at the wall-base (discussed later are the exceptions, models C1 and C4). For models F1 and F2, with a continuous wall-base joint, the bending moment at the wall-base is a positive value that is transferred into the base slab. The ring tension at the wall-base is also a positive value and a function of the self-weight settlement. The conical base tends to flatten and push out the wall-base joint, which generates ring tension forces.

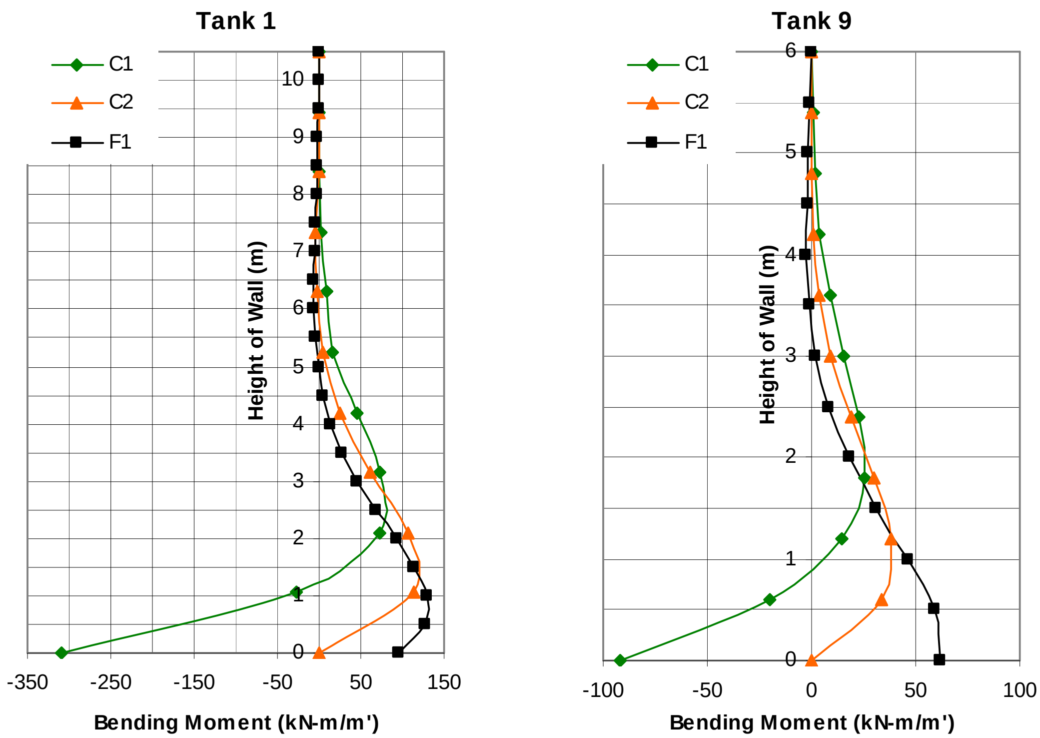

Figure 3: Bending moments in the tank wall (model F1 compared to C1 and C2)

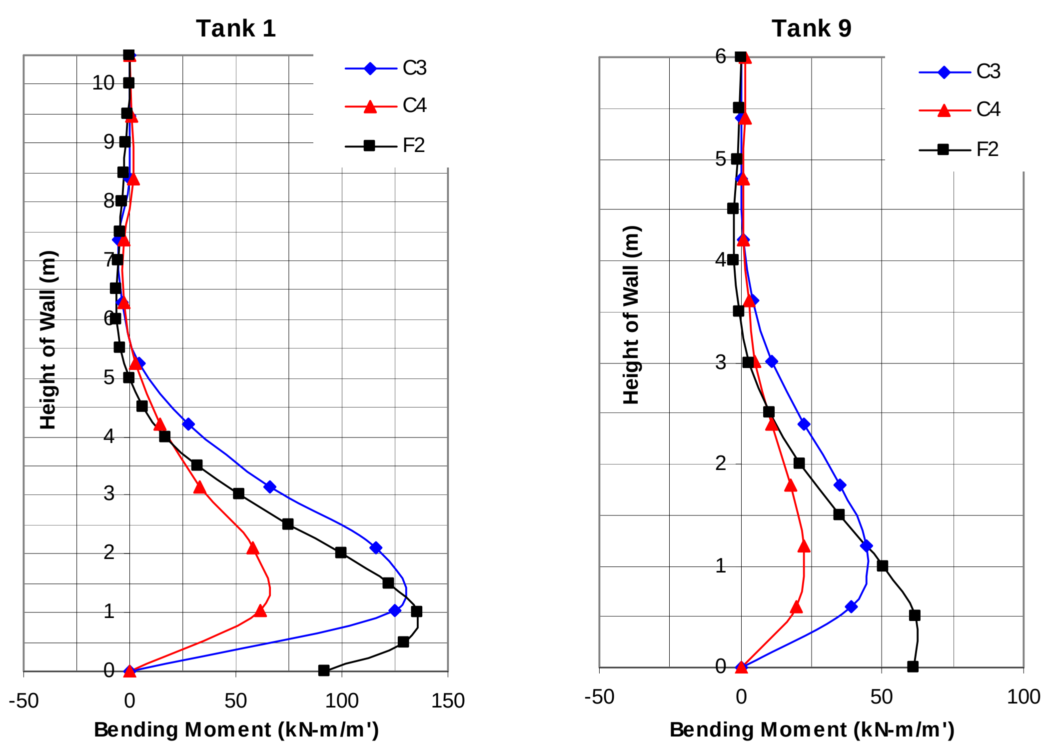

Figure 4: Bending moments in the tank wall (model F2 compared to C3 and C4)

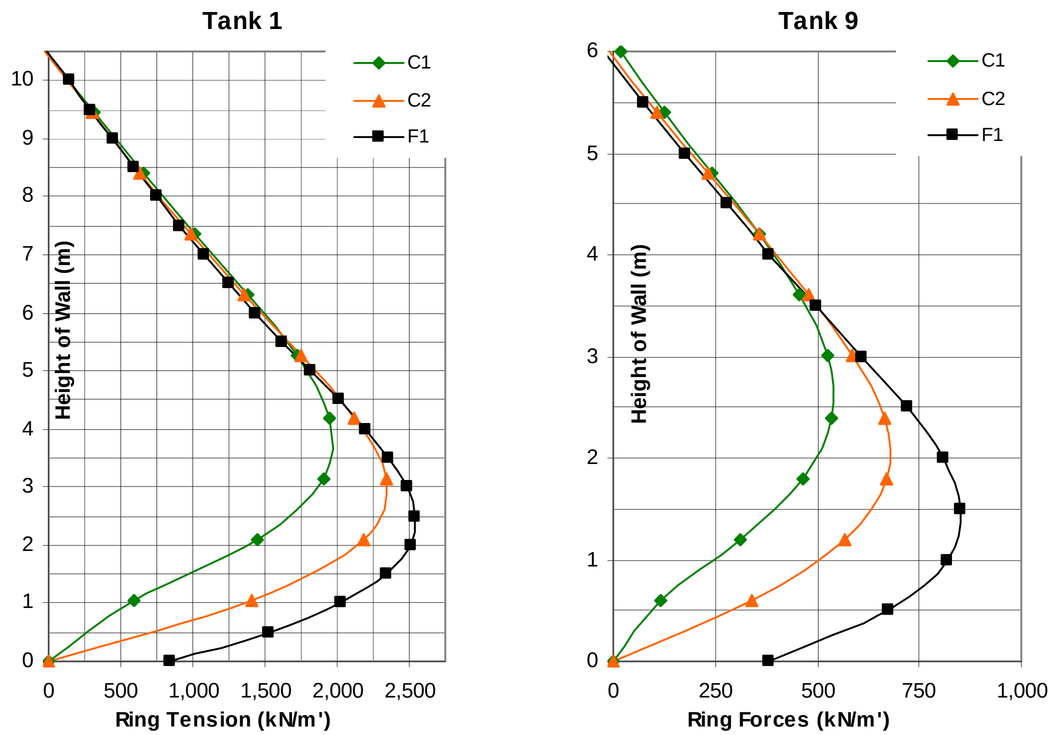

Figure 5: Ring Tension in the tank wall (model F1 compared to C1 and C2)

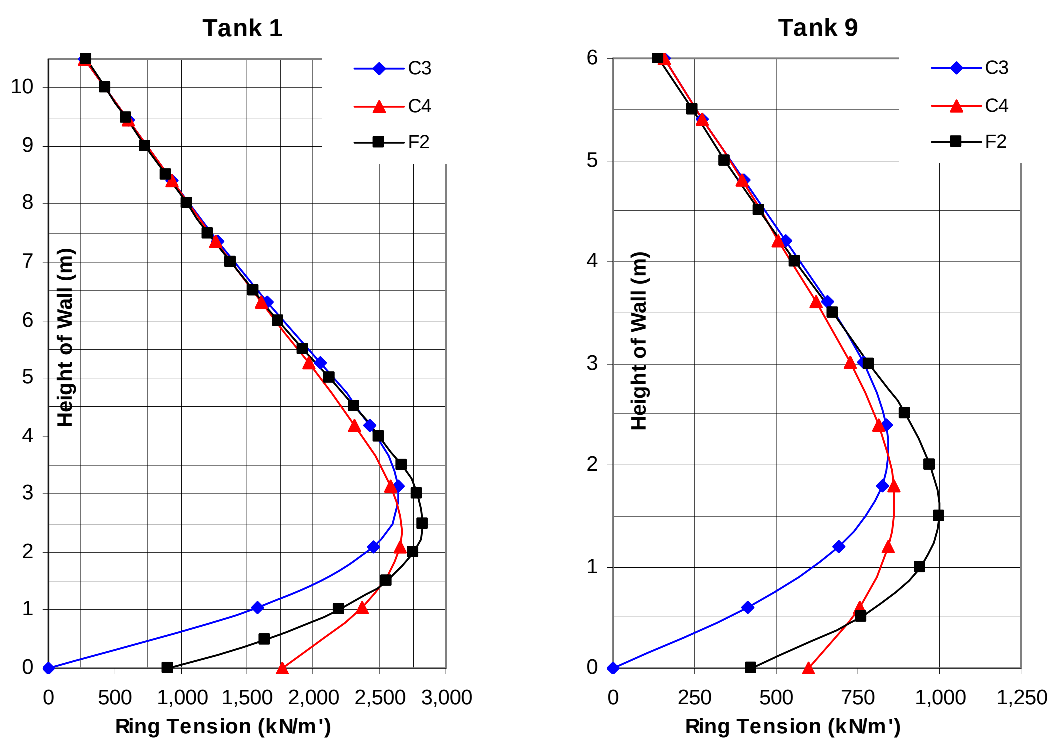

Figure 6: Ring tension in the tank wall (model F2 compared to C3 and C4)

6.1. Model C1 compared to F1

For bending moments in Figure 3 at the wall-base, model C1 generated large negative moments due to the fixed base boundary condition and F1 generated large positive moments due to moment distribution into the base slab. The shape of force diagrams from C1 and F1 are in good agreement within the upper two-thirds of the tank wall. From Table 3, the average IFD of maximum bending moments is -149% with an 8 percentage point standard deviation (ppsd). The average IFD is the largest of any model comparison of internal forces while the standard deviation is the smallest for bending moment. Notice that at the wall-base, model F1 has a positive value while C1 swerves largely negative. This was expected, as a perfectly fixed wall-base joint is unlikely in practice. Additionally, the largest positive bending moment from model F1 is larger than anywhere within C1. In the design of vertical reinforcement at the wall-base, it is important to determine which model represents how the tank will actually behave. Otherwise, the design may be highly inadequate.

For ring tension in Figure 5 at the wall-base, model C1 goes to zero due to the horizontally fixed base while F1 generated a positive tension due to the allowance of horizontal displacement. The shape of force diagrams from C1 and F1 are in good agreement within the upper half of the tank wall. From Table 3, the average IFD of maximum ring tension is 43% with a 7 ppsd. The average IFD is the largest of any model comparison of ring tension while the standard deviation is reasonably small. As explained earlier, under self-weight loading, the conical base tends to flatten and push out the wall-base joint which generates ring tension forces. Since model C1 is assumed to be fixed from horizontal displacement and rotation, it is understandable why the IFD are largest for this model comparison.

6.2. Model C2 compared to F1

For bending moments in Figure 3, model C2 goes to zero at the wall-base due to the hinged base boundary condition. The shape of force diagrams from C2 and F1 are in good agreement within the upper five-sixths of the tank wall. From Table 3, the average IFD of maximum bending moments is 19% with an 18 ppsd. Model C2 has the same applied loads as the fixed base model C1 but with drastically different internal forces. The average IFD is much smaller than model C1 while the standard deviation is large and nearly equal to the average IFD.

For ring tension in Figure 5, model C2 goes to zero at the wall-base due to the hinged base boundary condition. The shape of force diagrams from C2 and F1 are in good agreement within the upper half of the tank wall. From Table 3, the average IFD of maximum ring tension is 14% with a 5 ppsd. The ring tension increased with a hinged wall-base under the same loads as the fixed base model C1. Both the average IFD and standard deviation are smaller than model C1.

6.3. Model C3 compared to F2

For bending moments in Figure 4, model C3 goes to zero at the wall-base due to the hinged base boundary condition. The shape of force diagrams from C3 and F2 are in good agreement within the upper five-sixths of the tank wall. From Table 3, the average IFD of maximum bending moments is 11% with a 13 ppsd. The average IFD is the smallest of any model comparison of bending moment while the standard deviation is large and surpasses the average IFD.

For ring tension in Figure 6, model C3 goes to zero at the wall-base due to the hinged base boundary condition. The shape of force diagrams from C3 and F2 are in good agreement within the upper two-thirds of the tank wall. From Table 3, the average IFD of maximum ring tension is 11% with a 4 ppsd. The average IFD is smaller than model C2 while the standard deviation is the smallest of any model comparison of ring tension.

The only difference between models C3 and C2, and models F2 and F1, is the application of the surcharge load L2. Interestingly, the average IFD and standard deviation for bending moments and ring tension from model C3 are less than C2. This is because the internal forces for models “F” and “C” did not increase uniformly. As expected, load L2 is treated differently in CCT and FEA analysis tools.

6.4. Model C4 compared to F2

For bending moments in Figure 4, model C4 goes to zero at the wall-base due to the hinged base boundary condition. The shape of force diagrams from C4 and F2 are in good agreement within the upper half of the tank wall. From Table 3, the average IFD of maximum bending moments is 120% with a 25 ppsd. The average IFD is the second largest and the standard deviation is the largest of any model comparison of internal forces. The bending moment is reduced by half within the lower half of the tank wall due to the addition of load L3 to model C4. This load has the effect of pushing out the wall-base, which counteracts the natural outward rotation of the joint and reduces the bending moment. In the design of vertical reinforcement for the lower half of the tank, it is important to determine which model represents how the tank will actually behave. Otherwise, the design may be highly inadequate.

For ring tension in Figure 6, model C4 produces a very large positive force at the wall-base joint in response to the addition of load L3. The shape of force diagrams from C4 and F2 are in good agreement within the upper two-thirds of the tank wall. From Table 3, the average IFD of maximum ring tension is 8% with a 4 ppsd. The average IFD and standard deviation are the smallest of any model comparison of internal forces. In no case was the maximum ring tension from model C4 larger than F2, but the discrepancy at the wall-base warrants discussion. Recall that shear can only develop at the wall-base if it is restrained against horizontal displacement (otherwise, the reaction at the wall-base would be zero). As per CCT, the shear force the base can resist without moving horizontally is estimated for model C4. In Figure 6, it is clear that load L3 was overestimated.

7. SUMMARY AND CONCLUSIONS

For a fixed base model from CCT, El Mezaini (2004, 2006) found that the IFD between an FEA and CCT for maximum bending moment and ring tension forces in the tank wall were -151% and 59%, respectively. In this study, tank 9 with model C1 is comparable to El Mezaini with similar IFD of -168% and 59%. Note that for model C1, the average IFD of all nine tanks for maximum bending moment and ring tension forces in the tank wall is -149% and 43%, respectively. These numbers are lower than those found by El Mezaini.

The smallest IFD for maximum ring tension is found in model C4, but the IFD for maximum bending moment is very high. In models C2 and C3, the average maximum IFD for maximum bending moment and ring tension forces is small. This is the closest approximation of CCT to a more detailed FEA that considers the effects of self-weight loading, soil-structure interaction, and changes in base geometry.

For designers, it is recommended that an FEA be employed if the shape, load cases, and assumed boundary conditions of the tank in question fall outside the parameters outlined by CCT. Otherwise, the resultant internal forces from CCT may lead to an inadequate design. However, if a designer were to use an FEA with no prior modeling experience or context for the analysis output, then it is possible that misleading results might not be recognized as such. Thus, both CCT and FEAs can be useful tools, either separately or in conjunction, but only if applied properly.

For further research on this topic, it would be interesting to investigate the following: 1) quantify the percent contribution to the IFD from the individual effects of self-weight loading, soil-structure interaction, and changes in base geometry, and 2) determine whether a statistically significant variance in IFD exists in the wall and base slab between tanks with similar H, D, H^2/Dt, and D/H.

8. ACKNOWLEDGEMENTS

The author would like to thank the following individuals for their support: Tyler Lahti, John Slade, David O’Sullivan, Steven Bertolo, and Sasha Regehr.

9. REFERENCES

American Concrete Institute (ACI). 2005. *Building Code Requirements for Structural Concrete, and Commentary*. Report by ACI Committee 318, ACI-318-05, Detroit.

American Concrete Institute (ACI). 2006. *Code Requirement for Environmental Engineering Concrete Structures, and Commentary*. Report by ACI Committee 350, ACI-350-06, Detroit.

El Mezaini, N. 2004. *Analysis of Cylindrical Tanks with a Conical Base*. 5th Structural Specialty Conference of the Canadian Society of Civil Engineering, Saskatoon, Saskatchewan, Canada.

El Mezaini, N. 2006. *Effects of Soil-Structure Interaction on the Analysis of Cylindrical Tanks*. Practical Periodical on Structural Design and Construction, ASCE, February 2006, pg. 50-57.

Metcalf & Eddy. 1991. *Wastewater Engineering: Treatment, Disposal, and Reuse*. 3rd ed. McGraw-Hill, New York, NY, USA.

Portland Cement Association (PCA). 1993. *Circular Concrete Tanks Without Prestressing*. PCA, Skokie, Ill.

Water Environment Federation (WEF), American Society of Civil Engineers/Environmental and Water Resource Institute (ASCE/EWRI). 2010. *Design of Municipal Wastewater Treatment Plants; WEF Manual of Practice No. 8; ASCE Manuals and Reports on Engineering Practice No. 76. 5th ed.*, McGraw-Hill, New York, NY, USA.